JOURNAL OF MATERIALS SCIENCE 26 (1991) 743–748

Compatibility and morphology of blends of isotactic and atactic polypropylene

D. J. LOHSE
Corporate Research Laboratories, Exxon Research and Engineering Company, Route 22 East, Annandale, New Jersey 08801, USA

G. E. WISSLER *
Polymers Group Exxon Chemical Company, P.O. Box 5200, Baytown, Texas 77522, USA

The compatibility and morphology of blends of isotactic and atactic polypropylene have been studied by several means: X-ray scattering, differential scanning calorimetry, and electron microscopy. It was found that the atactic polymer was located mainly inside the spherulites of the isotactic polypropylene on a scale approximately equal to that of the crystalline lamellae. This means that these two polymers were more intimately mixed than are blends of polypropylene and ethylene–propylene copolymer, in which the location of the copolymer is unrelated to the spherulite structure. This difference can be explained by the fact that atactic and isotactic polypropylene are miscible in the melt, whereas polypropylene and ethylene–propylene copolymer are not.

1. Introduction

One of the characteristic features of polymers that arises from their structure as long chain molecules is that the entropy of mixing for a blend of two polymers is quite small. The result of this is that nearly all pairs of polymers are insoluble in each other [1]. Such immiscibility can even arise from small changes of polymer composition or molecular weight. Recent studies by both neutron and light scattering have shown that ethylene–propylene copolymers (EP) are not miscible with isotactic polypropylene (iPP) in the melt [2, 3]. This is true even when the ethylene content is as low as 12 wt% [2]. Atactic polypropylene (aPP) was, however, found to be miscible with iPP in the melt. The question then arises as to whether the difference in melt miscibility between EP–iPP blends and aPP–iPP blends leads to differences in the morphology of these blends below the crystallization temperature of iPP.

There are three main scales of structure in isotactic polypropylene, which are indicated schematically in Fig. 1. This means that there are several possible degrees of phase separation between aPP and iPP in such blends once the latter crystallizes. The largest scale is represented in Fig. 1 by a spherulite, which can be as large as 100 μm or greater in polypropylene, depending on the conditions of crystallization. One place in which aPP could be located in a blend is at the spherulitic boundaries, being completely excluded from the growing spherulites. At the next smaller scale are rods which grow radially from the centre of the spherulite and consist of stacks of lamellae. These have been described by Kojima [4], and some micrographs of these structures are shown below. It is also possible that the aPP is located in between the rods. The smallest scale shown is that of the crystalline lamellae. The aPP chains may also be in the amorphous region between the lamellae, if they have not moved very far during the iPP crystallization. It may even be possible that the aPP has cocrystallized with the iPP.

Little work has been reported in this area. Padden and Keith [5, 6] removed the heptane soluble fraction from a commercial polypropylene and then blended this material back into the crystalline polymer. This amorphous polypropylene was not completely atactic polymer but also contained some low molecular weight isotactic material. They provided crystallographic evidence that there was no cocrystallization of the two fractions, however, they were unable to exactly pinpoint the location of the amorphous component.

A similar study has been conducted on blends of atactic and isotactic polystyrene [7, 8]. The two forms of polystyrene were shown by neutron scattering to be compatible in the melt. X-ray scattering results suggested that segregation of the two components took place during crystallization on a scale larger than the lamellae but smaller than the spherulites.

In this paper, we report the results of X-ray scattering, differential scanning calorimetry, and

* *Present address*: Exxon Chemical Company, Al-Jubail Petrochemical Company, PO Box 10084, Madinat Al-Jubail Al-Sinaiyah 31961, Saudi Arabia

0022–2461/90 $03.00 + .12

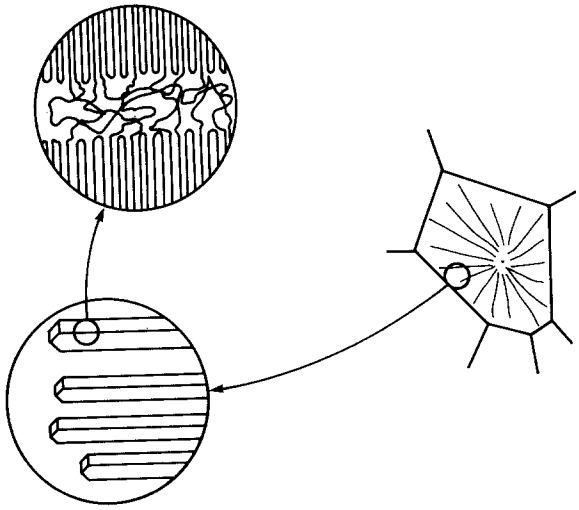

Figure 1 The structure of semi-crystalline polypropylene at various size scales.

electron microscopy work aimed at finding out where atactic polypropylene is located in a blend with isotactic polypropylene.

2. Experimental details

2.1. Polymers

In order to test the role of tacticity in blend compatibility, it is important to have a truly atactic polypropylene, rather than simply an amorphous one. Therefore, some polypropylene was made expressly for this work using the soluble catalyst system of vanadium tetrachloride and diisobutyl aluminium chloride. The polymer made from this catalyst has been labelled PPA. Polypropylenes made in this way were shown by ^{13}C-NMR to be truly atactic (that is, equal amounts of meso and racemic dyads). This catalyst system also allows for the preparation of atactic polymer with fairly high molecular weight, as shown in Table I; other soluble catalysts produce polypropylenes of much lower molecular weight. The isotactic polymer, PPI, is an Exxon Chemical Co. commercial grade. Characterization data for both polymers may be found in Table I.

TABLE I Molecular weight characteristics of polymers used

Polymer	M_n ($\times 10^4$)	M_w ($\times 10^4$)	M_w/M_n	Tacticity
PPA	0.578	8.57	14.79	Atactic
PPI	9.21	55.4	5.29	Isotactic

As measured by GPC.

2.2. Blending

Blends of these two polymers were made both in solution and in the melt at compositions ranging from 90 PPI–10 PPA to 25 PPI–75 PPA (by weight). The solution blending was performed by dissolving both components in hot 1,2,4-trichlorobenzene, holding at 200 °C for 2 h, and then precipitating into methanol at 2 °C. Melts blends were made in the CSI-MAX® Mixing Extruder CS-194, based on Maxwell's ideas for a screwless extruder [9]. No significant differences were seen between the two sets of blends in the study described herein, so in general the blending procedure is not specified.

2.3. Differential scanning calorimetry

All of the blends were run on a Perkin-Elmer DSC-2 to measure their glass transition and melting temperatures. Samples of from 3 to 5 mg were first heated to 490 K, then cooled at 10 K min^{-1} to 220 K. DSC scans were then recorded at 10 K min^{-1}. The melting point is defined as the peak of the melting endotherm. Heats of fusion are calculated from the area under the DSC peak and are reported on the bases of both total weight and isotactic weight fraction. These results are presented in Table II and Fig. 2.

2.4. X-ray scattering

Compression-moulded films, approximately 125 μm thick, were prepared for wide and small X-ray scattering measurements. Wide angle X-ray diffraction patterns were recorded with nickel-filtered copper K_α radiation from a Rigaku horizontal diffractometer. Small angle X-ray scattering patterns were recorded on a Tennelec position sensitive detector, using 0.2 mm diameter pinholes and vanadium-filtered chromium K_α radiation from a Rigaku rotating anode, operated at 40 KV and 100 mA. The sample to detector distance was 425 mm. This distance was evacuated to minimize air scattering. By stacking films

TABLE II DSC data for PPI–PPA blends

Composition	T_{max}[a] (K)		Heat of Fusion, ΔH_F			
			Absolute (cal qm^{-1} total)		Relative (cal qm^{-1} iPP)	
(wt% PPA)	Melt blend	Solution blend	Melt blend	Solution blend	Melt blend	Solution blend
10	435.34	438.28	17.47	21.11	19.41	23.46
20	434.75	435.80	17.26	17.08	21.58	21.35
30	433.57	435.90	16.00	15.30	27.86	21.86
40	433.20	434.71	12.90	13.12	21.50	21.82
50	432.57	433.35	11.95	11.51	23.90	23.02
75	431.04	431.35	6.54	5.76	26.16	23.04
					Average = 22.43 ± 0.32	

[a] Temperature at maximum in melting peak.

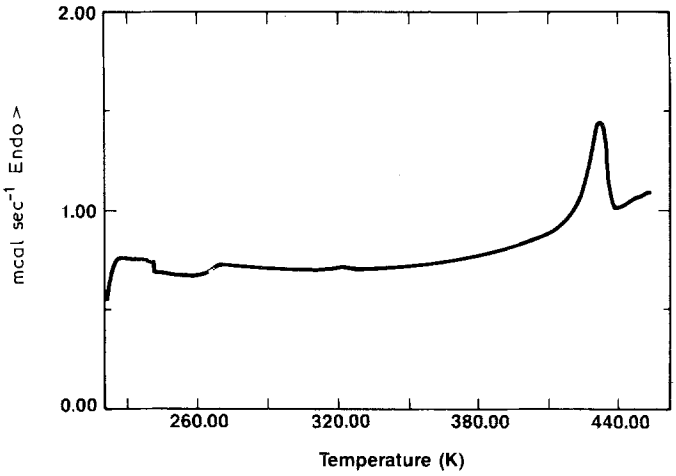

Figure 2 DSC thermograms for 25 PPI–75 PPA melt blend.

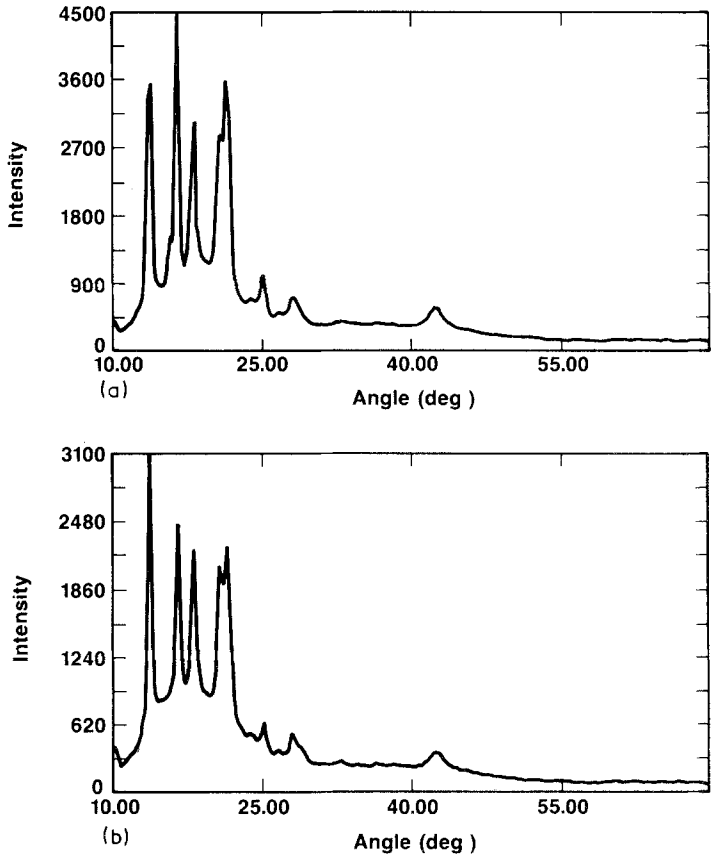

Figure 3 Wide angle X-ray scattering functions. (a) PPI; (b) 70 PPI–30 PPA melt blend.

to obtain an optimum sample thickness of about 1 mm, acquisition times of about 4 h resulted. An example of the WAXS data is shown in Fig. 3.

2.5. Electron microscopy

The morphology of these blends was imaged by extraction of the soluble PPA, so it was important to prepare the samples with no voids. This was done in two ways. To make the "fast-cooled" samples, approximately 0.1 g of the blend was vacuum moulded to produce a pellet 1 cm in diameter and about 1 mm thick. Cooling was performed fairly rapidly by running cool water through the moulding press. The "slow-cooled" samples were put into a vacuum oven, melted and then allowed to cool slowly (usually overnight). In both cases, the samples were sectioned using a Reichert-Jung FC-4 ultramicrotome, and the hexane soluble material was extracted at room temperature in a sonic bath, thus, the material remaining after extraction was the PPI, and the holes showed where the PPA had been. A JEOL 35C scanning electron microscope was used to examine the prepared samples.

Figure 4 SEM micrographs of vacuum moulded PPI, 45° tilt.

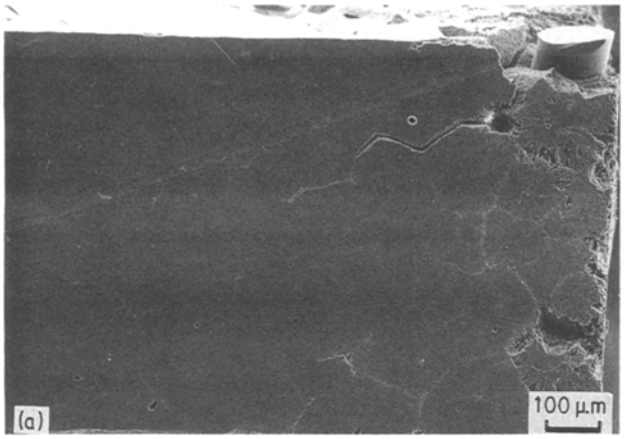

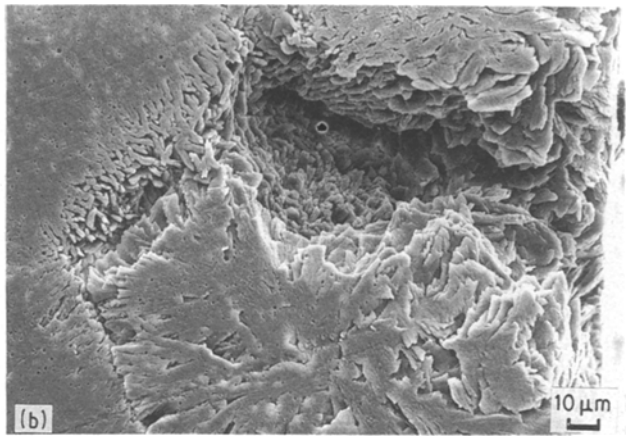

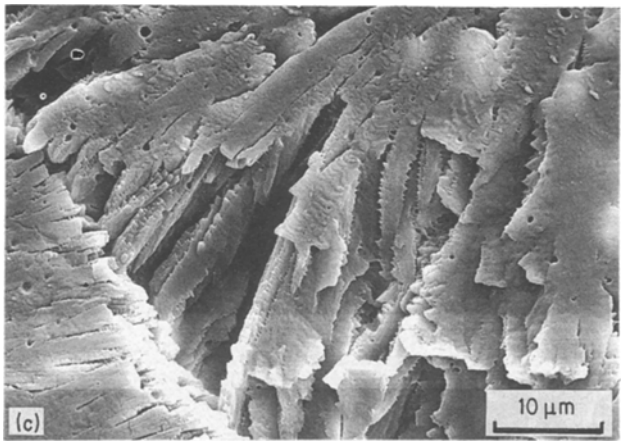

Figure 5 SEM micrographs of slow-cooled 90 PPI–10 PPA melt blend. a.c. no tilt.

3. Results

3.1. Differential scanning calorimetry

A typical DSC scan, here from the 25 PPI–75 PPA blend, is shown in Fig. 2. The most prominent feature is the melting peak near 431 K, and the glass transition in the PPA can also be seen around 270 K. The results from all the samples are compiled in Table II. There was very little change in the melting temperature of the PPI with composition, and similarly the heat of fusion per gram of PPI was quite constant. Thus, there was no cocrystallization between the components.

3.2. X-ray scattering

The absence of cocrystallization was confirmed by wide angle X-ray scattering. The scattering patterns of a straight polypropylene sample and that from a 70 PPI–30 PPA blend are shown in Fig. 3. The scattering peaks were all at the same angles, meaning that the lattice parameters of the PPI crystals were unchanged upon blending, thus, the PPA did not cocrystallize with the PPI.

At smaller angles the scattering arises from larger structures. Some small angle X-ray scattering data was taken at angles corresponding to the lamellar spacing in polypropylene crystallites. For both a straight PPI sample and a 90 PPI–10 PPA, this spacing was found to be 11.1 nm. This peak was not resolved in blends with higher PPA content. The SAXS patterns indicate a continuous increase in the long period with increasing atactic content. This is demonstrated by changes in both the shape and angular positions of the scattering profiles. To examine larger sizes, it is necessary to use electron microscopy.

3.3. Electron microscopy

Figs 4 to 10 show the morphologies of a number of the blends we have examined, which vary in composition and preparation. As stated above, all were microtomed and then the PPA was removed with hexane. Samples of several compositions and preparations were examined without extraction, and essentially no voids were present. We are, thus, confident that the holes in these micrographs represented the PPA, while the remaining material was the PPI.

Fig. 4 shows the base case, a sample of 100% PPI. This was nearly featureless except for some knife marks. By tilting the sample 45° to bring out the surface texture, a slight indication of the spherulite morphology can be seen.

The sample shown in Fig. 5 was a 90–10 blend of the PPI and PPA which was cooled slowly in the oven (see above). The free surface of the blend during heating and cooling is on the right-hand side of Fig. 5a. The spherulites are clearly visible, since some of the material had been extracted from the spherulite boundaries. There also seems to have been more PPA at the free surface of the sample since much more material was extracted from there, because of this the internal structure of the spherulites can be seen. Fig. 5b shows a spherulite near the surface. The internal structure of the spherulite as rods emanating from its center is clear and quite similar to that shown by Kojima [4] in blends of PPI and paraffins. These rods are shown in more detail in Fig. 5c. They probably consisted of stacks of lamellae.

The morphology of a solution blend of the same (90–10) composition which was vacuum moulded is shown in Fig. 6. The spherulite seen here is much smaller than that in, say, Fig. 5b. This is because of the faster cooling used for the moulded sample as discussed above. In fact, the sizes of the spherulites did not differ significantly between the blends of different compositions, but did depend on the rate of cooling.

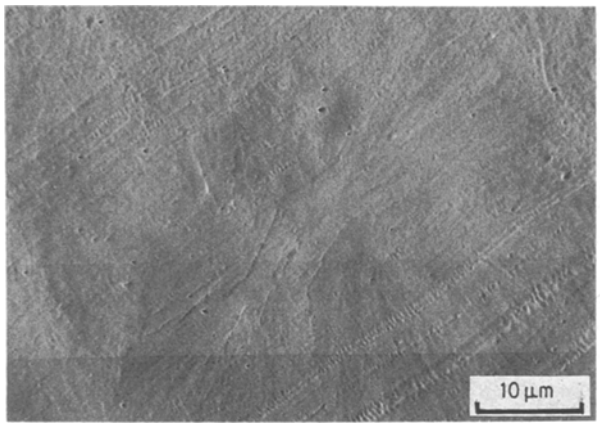

Figure 6 SEM micrograph of vacuum moulded 90 PPI–10 PPA solution blend, 45° tilt.

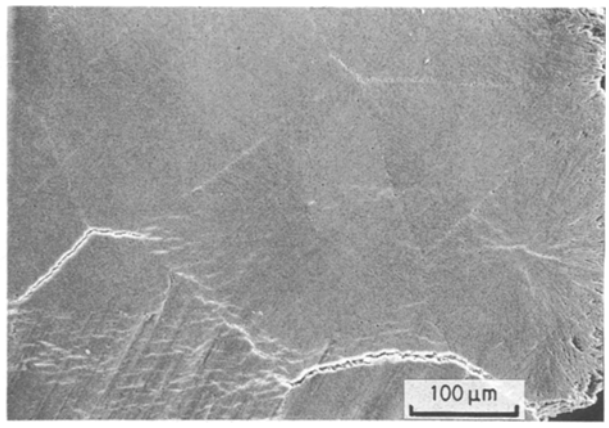

Figure 8 SEM micrograph of slow cooled 60 PPI–40 PPA melt blend, 45° tilt.

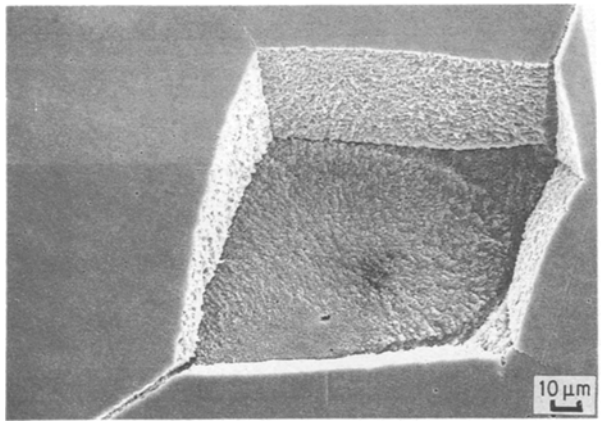

Figure 7 SEM micrograph of slow-cooled 80 PPI–20 PPA melt blend, no tilt.

Figure 9 SEM micrograph of vacuum moulded 50 PPI–50 PPA melt blend, 45° tilt.

This can be seen in Fig. 7 (80 PPI–20 PPA) to 10 (25 PPI–75 PPA). Moreover, as the content of PPA in the blends increased, the visibility of the spherulites also increased. Fig. 8 also shows a hole from which a spherulite has fallen out. This made visible the surfaces of the adjoining spherulites. Once more, the tips of the rods can be seen on these surfaces.

The results in Fig. 10 on the low PPI content blend (25–75) were surprising in that the sample did not fall apart upon extraction. The spherulites still spanned the system. Clearly, a large amount of material had been extracted from the blends but they still held together. The sizes of the spherulites were also quite similar to those in the blends of higher PPI content.

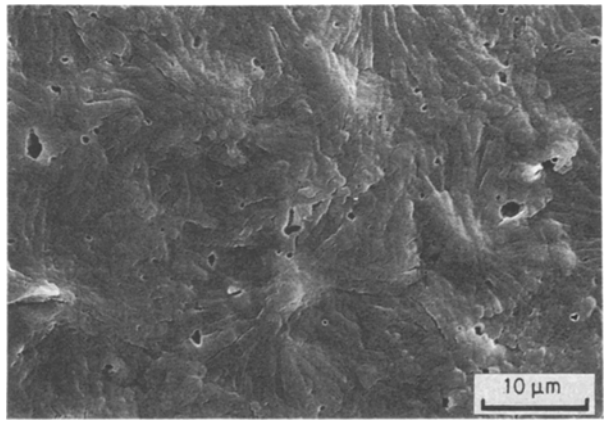

Figure 10 SEM micrograph of vacuum moulded 25 PPI–75 PPA melt blend, no tilt.

4. Discussion

From the data presented above, it is clear that the atactic polypropylene resided mainly inside the spherulites, both between the rod-like structures which project radially from the centres of the spherulites and between the lamellae. This was true at all levels of atactic polymer content in the blend. There did seem to be a small amount of polymer dispersed in domains unconnected with the spherulites, as well as a small amount at the spherulitic boundaries. The X-ray data showed that some of the atactic polypropylene was interlamellar, and certainly none cocrystallized with the isotactic polymer. The large majority is found associated with the rods, which was most clearly demonstrated by remarkable imaging of the spherulites in the extracted blends.

This is different from the morphology found in blends of isotactic polypropylene and ethylene–propylene copolymers. In these blends the copolymer is almost always found in disperse spherical domains [10–16], and there is some evidence that the EP domains can nucleate the polypropylene spherulite [15]. However, in general the distribution and sizes of

the EP phase domains seem to be unrelated to the spherulitic structure of the polypropylene [14].

This difference between the morphology of aPP–iPP blends at room temperature and that of EP–iPP blends can be related directly to the difference in their miscibility in the melt [2, 3]. The atactic and isotactic polypropylenes are miscible at high temperatures, thus they are mixed quite intimately even after crystallization of the iPP. The atactic chains are rejected from the interlamellar regions, but not much further. In contrast, the EP and iPP are phase separated in the melt, and these domains will grow as long as the blend is held in the melt. This produces the sort of phase dispersion more usually seen in polymer blends thus, this is an example of how small differences in polymer molecular structure can lead to large differences in miscibility and so in blend morphology and physical properties.

Acknowledgements

Special thanks are due to S. Datta who synthesized the atactic polypropylene used in this work. The blends were made by W. D. Gallagher and E. Janiec, while the electron microscopy was performed by L. L. Ban and J. H. Oskam. This work was also aided by helpful discussions with M. J. Doyle and F. C. Stehling.

References

1. S. KRAUSE, In "Polymer Blends", edited by D. R. Paul and S. Newman (Academic Press, New York, 1978) p. 15.
2. D. J. LOHSE, *Polym. Engng Sci.* **26** (1986) 1500.
3. N. INABA, K. SATO, S. SUZUKI and T. HASHIMOTO, *Macromolecules* **19** (1986) 1690; N. Inaba, T. Yamada, S. Suzuki, and T. Hashimoto, *ibid.* **21** (1988) 407.
4. M. KOJIMA, *J. Polym. Sci. Lett.* **17** (1979) 609.
5. F. J. PADDEN, JR. and H. D. KEITH, *J. Appl. Phys.* **30** (1959) 1479.
6. H. D. KEITH and F. J. PADDEN, JR., *ibid.* **35** (1964) 1270.
7. F. P. WARNER, W. J. MacKNIGHT and R. S. STEIN, *J. Polym. Sci. Phys.* **15** (1977) 1270.
8. M. P. WAI, PhD Thesis, University of Massachusetts, Amherst (1982).
9. B. MAXWELL, *Plastics Engng* **3065** (1974) 40.
10. R. C. THAMM, *Rubber Chem. Tech.* **50** (1977) 24.
11. K. C. DAO, *Polymer* **25** (1981) 1527.
12. J. KARGER-KOSCIS, L. KISS and V. N. KULEZNEV, *Polymer Commun.* **25** (1984) 97.
13. J. KARGER-KOSCIS, A. KALLO and V. N. KULEZNEV, *Polymer* **25** (1984) 279.
14. B. Z. JANG, D. R. UHLMANN and J. B. VANDER SANDE, *J. Appl. Polym Sci.* **29** (1984) 4377.
15. E. MARTUSCELLI, C. SILVESTRE and L. BIANCHI, *Polymer* **24** (1983) 1458.
16. D. YANG, D. ZHANG, Y. YANG, Z. FANG, G. SUN and Z. FENG, *Polym. Engng Sci.* **24** (1984) 612.

Received 7 November 1989
and accepted 28 March 1990